ELSEVIER

Journal of Chromatography A, 911 (2001) 147–166

JOURNAL OF CHROMATOGRAPHY A

www.elsevier.com/locate/chroma

Phenomenological study of the bed–wall friction in axially compressed packed chromatographic columns

Djamel E. Cherrak[a,b], Georges Guiochon[a,b,*]

[a]*Department of Chemistry, The University of Tennessee, 552 Buehler Hall, Knoxville, TN 37996-1600, USA*
[b]*Chemical and Analytical Sciences Division, Oak Ridge National Laboratory, Oak Ridge, TN 37831-6120, USA*

Received 16 October 2000; received in revised form 22 December 2000; accepted 22 December 2000

Abstract

The properties of column beds prepared with slurries of Kromasil C_8 in 12 different solvents, using the same axial compression skid, were investigated. The extent of the consolidation of the column beds, their permeabilities, and the friction shear stress of these beds against the column wall were determined, as well as the column efficiencies (for an unretained tracer). The results of this study illustrate the influence of the wall effect on the consolidation. The permeability of columns consolidated under a constant compression stress was found to increase with increasing bed length. The bed–wall friction shear stress increases rapidly with increasing bed length and varies widely with the nature of the solvent used. No correlation was found between this shear stress and any physico–chemical property of the solvent. The best efficiency was observed for a column consolidated from a slurry in ethanol. © 2001 Elsevier Science B.V. All rights reserved.

Keywords: Axial compression; Wall effects; Shear stress; Stationary phases, LC; Column packing

1. Introduction

Highly efficient columns are required for the analytical separations of complex mixtures, for the preparative separations of closely related isomers, or for the purification of many chemical intermediates in the pharmaceutical industry. The efficiency needed is obtained by the suitable combination of an appropriate column length and of the height equivalent to a theoretical plate (HETP) that can be achieved with the packing material and the column-packing procedure available. As long as it is feasible to operate the column at the required mobile-phase flow velocity, hence to afford the corresponding inlet pressure, the analysis time decreases with decreasing HETP [1] and the production rate in all preparative applications increases [2]. These variations are rapid and provide a strong incentive to improve our packing procedure and to reduce the minimum HETP of the columns. Another requirement that has always been important for analytical columns is the reproducibility of their performance, also strongly dependent on the packing procedure. This requirement did not use to be as important for preparative columns because such columns are less often replaced and, within reasonable limits, it is easy to adjust the operating conditions that allow the achievement of

*Corresponding author. Department of Chemistry, The University of Tennessee, 552 Buehler Hall, Knoxville, TN 37996-1600, USA. Tel.: +1-865-9740-733; fax: +1-865-9742-667.
E-mail address: guiochon@utk.edu (G. Guiochon).

0021-9673/01/$ – see front matter © 2001 Elsevier Science B.V. All rights reserved.
PII: S0021-9673(01)00518-0

suitable results with a column having somewhat different properties. The increasing popularity of simulated moving bed chromatography, however, makes necessary the production of sets of columns having very close properties [3,4].

In order to reproducibly to pack high efficiency columns, it is critical to control every aspect of the packing procedure [5–18]. The consolidation of beds of rigid particles (silica-based material) in dynamic compression columns has been abundantly discussed [10–22]. It was shown that the average packing density of a bed is affected by the nature of the slurry solvent used to disperse the packing material, by the shape and size of the particles of this material, by the intensity of the mechanical stress applied against the bed and by the speed at which this stress is raised [10–18]. The packing density increases with increasing stress, whether axial [10–20] or radial [21,22] compression is applied to the column bed but it is not or it is only weakly correlated with a high column efficiency [16]. Measurements of the local values of the packing density and of other column properties show that both analytical and preparative columns are radially heterogeneous [23–26]. Due to the finite amplitude of the radial distribution of the porosity of the column, hence of its permeability, the zone of a compound migrates at a different velocity in the column center or close to the wall. It becomes warped. Because the width of the eluted band is measured in the bulk stream of the eluent leaving the column and fractions are collected from this stream, the warping of the bands results in a relatively poor apparent column efficiency.

Friction of the bed against the wall of the column explains this radial heterogeneity. The column wall supports the bed of packing material and, in the process, causes radial and longitudinal heterogeneity of this bed [19]. As a consequence, the packing density decreases, hence the permeability increases from the wall toward the center of the packed bed and from the top of the column toward the region close to the piston where the intensity of the compression stress is higher (assuming that compression takes place from the bottom up). For the same reason, the bed remains stuck to the column wall, it cannot contract freely when the inlet pressure increases, and the mobile phase cannot leak around it [19]. This phenomenon is known as the ''wall effect'' in both chromatography [23–26] and chemical engineering [27–30].

Zou and Yu studied the wall effect on the packing of spherical [27] and cylindrical [28] particles, using glass beads (1 to 12 mm in diameter) and marble balls (16 to 37 mm) in the former case, wooden rods (2.35 mm in diameter, 1 to 64 times as long) in the latter. They showed a strong influence on the average bed porosity of the ratios d/D and d/H of the bead (or rod) diameter (d) to the column diameter (D) and the column height (H). No discussion of the radial distribution of the local porosity was provided, however. Their results are difficult to apply to chromatographic beds because the typical values of the two ratios above for our own experiments (see later) are $2\cdot10^{-4}$ and $7\cdot10^{-5}$, respectively, while the smaller values for which Zou and Yu obtained experimental results were $2\cdot10^{-2}$. At the lowest values of these ratios, the porosity was between 0.37 (densest packing) and 0.40, a range slightly lower than that within which most data for chromatographic columns are found. Note, however, that for beds packed with large size beads of glass or marble, the contribution of gravity to the mechanical stress is important.

Although the physical laws applying to particle beds are the same for analytical and preparative columns, the different principles on which are based the packing procedures used to prepare them justify separate studies. We are concerned here only with columns packed by dynamic axial compression. The goal of this work was to investigate the influence of the nature of the slurry solvent on the performance of chromatographic columns the beds of which were consolidated under axial compression stress. This study builds on previous results [19] that demonstrated the importance of the friction of the bed against the wall on the homogeneity of chromatographic columns. The intensity of this friction appeared to depend considerably on the nature of the solvent used to pack the column, as well as, more expectedly, on the intensity of the axial compression stress applied to the bed and on its length [19]. The performance of the column beds consolidated from slurry dispersions prepared with different solvents was also investigated.

2. Experimental

2.1. Equipment and materials

2.1.1. Instruments

An LC-50 dynamic compression column skid (Prochrom, Champigneulles, France) was used to prepare and operate dynamic axial compression columns [10]. The packing material is compressed by a piston moving inside a cylinder actuated by a hydraulic jack. The column body is a stainless steel cylinder 5 cm I.D., designed to allow a maximum hydrostatic pressure of approximately 100 kg/cm^2. The column walls are polished, with an RA (arithmetic mean roughness value) between 0.2 and 0.4 μm [13]. A series of chevron seals prevent leaking between the piston and the wall of the column. A newly designed piston head supplied by the manufacturer allowed an easier cleaning of the frits and afforded reduced extra-column contributions to band broadening.

A Dynamax SD1 (Rainin, Woburn, MA, USA) pump equipped with dual pistons was used as the solvent delivery system, with a maximum flow-rate of 800 ml/min and a maximum pressure of 1500 p.s.i. (ca. 105 bar). The UV detector was a SpectraFocus (Thermoseparation Products, Riviera Beach, FL, USA) equipped with a preparative flow cell (optical path length, 2.8 mm throughout all the experiments reported here). The UV signal was recorded at a wavelength of 254 nm (unless otherwise specified). A six-port electro-pneumatic switching valve was used to inject the sample. For all the experiments, the sample volume was 0.5 ml. The special top flange described earlier [19], fitted with a 30 mm extension, was used during these experiments to allow us to carry out both the determination of the column characteristics and the friction measurements, without having to disturb or move the consolidated bed.

The column inlet pressure (ΔP) was measured with an Omega pressure transducer Model PX603-2KG5V (Stamford, CT, USA). This transducer allows the measurement of pressures up to 140 bar with a response time of 1 ms. Dynamic changes of the column length smaller than 1 cm (accuracy, 0.01 mm) were measured with an Electro-Mike displacement sensor Model PAA1555 (Reagan Controls, Charlotte, NC, USA) which includes a displacement transducer and a transmitter with an analog output. Larger changes were derived from the displacement of an index fixed on the piston, measured with a ruler (accuracy ca. 1 mm). The electrical signals of the displacement sensor, the pressure transducer, and the UV detector were collected with the data acquisition system Maxima 820, version 3.3 (Waters, Milford, MA, USA). All the data files were translated into ASCII format and downloaded to one of the computers of the University of Tennessee Computer Center for further data processing.

A 250×4.6 mm analytical column was packed in our laboratory, using the same packing material as for the preparative column and a conventional slurry packing method (in methanol) at 300 bar. The characteristics of this column were measured with a HP1090 liquid chromatograph (Hewlett-Packard, Palo Alto, CA, USA) equipped with a ternary solvent delivery system and a diode array UV detector.

2.1.2. Packing material

All the columns studied were packed with Kromasil C_8, a silica-based material for reversed-phase liquid chromatography (RPLC) (spherical particles, average diameter, 10 μm) from Eka Chemicals (Akzo Nobel, Bohus, Sweden).

2.1.3. Mobile phase and chemicals

Dilute solutions (concentration lower than 0.2 g/l) of uracil, thiourea (Aldrich, Milwaukee, WI, USA) or HPLC-grade toluene (Fisher Scientific, Fair Lawn, NJ, USA) were injected to measure the column efficiency and the retention volume, hence the total column porosity. The compounds used as packing solvents and mobile phases in this study, acetone, acetonitrile, chloroform, ethyl acetate, ethylene glycol, ethanol, *n*-hexane, isopropanol, methanol, *n*-octanol, methylene chloride, tetrahydrofuran (THF), and water were all HPLC grade or analytical grade. All the chemicals and solvents were used without further purification.

2.2. Procedures

2.2.1. Column packing and consolidation

All chromatographic columns were packed following the same procedure as previously described [8–12,15–17]. The exact amount (60 g, unless specified otherwise) of dry packing material required was mixed with 200 ml of the selected solvent and turned into a thick slurry. The concentration of the slurry (ratio of dry-packing mass to total volume of solvent) was kept constant for all the columns. The slurry was stirred for several minutes in an ultrasonic bath and rapidly poured into the empty column. The column was closed and the axial compression stress was rapidly applied to the column, up to the desired value (in most cases, 40 bar). This axial compression stress was lower than the one used in most of our previous studies. It was chosen (1) to minimize the extent of particle breakage during the consolidation [13,17], even with particles as strong as those of Kromasil used here, (2) because the bed length corresponding to the mass of packing material selected was also unusually short, and (3) because most users prefer this lower level of stress. The variation of the bed length was recorded during the consolidation step, at constant compression stress. After the consolidation of the column had taken place, the compression stress was abruptly released and the new bed length recorded, in order to measure the elastic reaction of the packed bed. This relaxation provides information on the behavior of the packing consolidated under a given stress [19].

Before each new experiment, the column and its frits (bottom and top of the column, at the top of the piston and under the top flange, respectively) were carefully cleaned (Fig. 1). The fine mesh grids of the frit keep the packing particles from flowing out of the column and allow the homogenous distribution of the flow pattern over the column cross-section. However, particle breakage takes place to some extent during the consolidation of packing materials under high compression stress, even for strong spherical particles. The fines made by the broken particles are produced where the mechanical stress is highest [13,35], in a wedge against the piston and close to the column wall. Part of them are encrusted inside meshes of the grid at the time of particle breakage. Others migrate along the column and get trapped inside the outlet grid. Abrasion during handling of the packing material results also in some particle fragmentation, even with spherical particles. In all cases, these fines cause partial obstruction of the exit frit (i.e., pore clogging) and an uneven flow distribution. The frits were periodically soaked in methanol and irradiated for 30 min in an ultrasonic bath. This procedure allows a faster cleaning and a better removal of the fine particles.

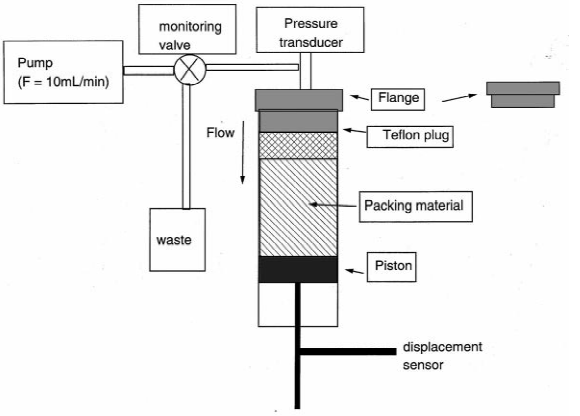

Fig. 1. Schematic design of the equipment for the measurement of the bed–wall friction shear stress.

Because of the limited amount of packing material available, we had to reuse it for most of the experiments reported here. After all the measurements and experiments had been carried out on a given column, it was unpacked and the material recovered was suspended in methanol. The fines resulting from particle breakage during consolidation and unpacking were removed and the material dried. Its amount was adjusted for packing the next column. The same lot of packing material was not used more than three times.

2.2.2. Measurements of column characteristics

For most columns packed as just described, the kinetic of consolidation, the permeability, and the column efficiency of the consolidated bed were measured. The permeability was derived from measurements of the column inlet pressure at different mobile phase flow-rates ranging from 1 to 100 ml/min. The column efficiency was determined from the maximum of the peak of thiourea (or uracil) and its width at half-height. A correction was applied for the

extra-column contribution to band broadening. The value measured with the unmodified instrument was large. The piston head was replaced. At that time, it was noted that when the piston head was raised to its top position in an empty column, there was still a 2 mm deep gap between the column outlet frit and the top of the piston head. During direct measurements of the extra-column contribution, this void behaves as an important mixing chamber, hence causes an overestimate of the extra-column variance contribution. The difficulty was overcome by filling the void with enough packing material (ca. 3 mm bed length) and measuring the variance of the sample, now taken as the correction. The extra-column variance decreased exponentially with increasing mobile phase flow-rate (results not shown). Note that the inlet and outlet frits are the major cause of the extra-column variance.

For all the HETP measurements reported here, the column was packed with 240 g of Kromasil C_8 and consolidated under a stress of 40 bar for a few hours. After consolidation, the slurry solvent was replaced by flushing the column with a few column volumes of pure methanol (N.B. the column consolidated in *n*-hexane was first flushed with ethanol because *n*-hexane is poorly soluble in methanol). The efficiency was determined from the peaks of thiourea and 1-phenyltridecane (PTD, $k'=1.2$).

The HETP was measured at several flow-rates and the result corrected as explained. It was plotted versus the reduced velocity ($\upsilon = ud_p/D_m$, with u the linear or superficial velocity, or ratio of the mobile phase flow-rate to the cross-section of the column, d_p the average particle diameter, and D_m the molecular diffusivity). This last coefficient was estimated for the compounds used in this study, using the classical Wilke–Chang equation [31]. The reduced velocities and the actual reduced plate heights were fitted to the Van Deemter equation [32], using a nonlinear least-squares fit.

2.2.3. Friction measurements

After completion of the determination of the column characteristics, the friction between the consolidated bed and the column wall was measured, following the procedure previously described [19], by extruding the bed out of the column (see Fig. 1). During this experiment, a leakproof plug, 25 mm × 49 mm O.D., made of a stainless steel cylinder bolted to two PTFE disks, was placed on the top of the packing material, inside the column, in place of the special top flange [19]. The use of this fixture avoids moving the bed and affecting the texture or the morphology of the cake by changing the orientation of the particles. This PTFE plug and the consolidated packing material can then be pushed together by pumping methanol through the top of the column, above the plug. This solvent cannot reach the packing material, mix with the packing solvent and possibly change the bed composition or its cohesion, or erode the bed. The bed was then reconsolidated under 40 bar, after what the axial compression stress was released, the compression piston let free to slide along the cylinder and methanol was pumped into the top of the column, at a flow-rate of 10 ml/min, with a pressure-controlled leak. The pressure was increased stepwise through an adjustable valve. The pressure of the liquid above the plug and the displacement of the axial compression piston were recorded (see Fig. 1). The intermediate plateaus during the progressive increase of the shear stress applied to the bed–wall junction were made as attempts to test the stability of this junction over time.

3. Results and discussion

3.1. Compressibility and compression kinetics

Fig. 2 shows plots of the bed length versus time after application of the axial compression stress to the column bed (solid lines, compression) and after release of this stress (dotted lines, relaxation). For the sake of clarity of these plots, the compression stress was applied only after the displacement signal had been recorded for 1 min (baseline). The bed length drops rapidly following the rapid application of the compression stress (ca. 40 bar), then slows down quickly and stabilizes. An occasional second collapse of small amplitude may be observed about 15 min after application of the compression stress. For columns packed with 30, 60, 120, 180 and 240 g in methanol, almost all the extent of the consolidation took place during the first few seconds (data not shown). Regardless of the amount of packing materi-

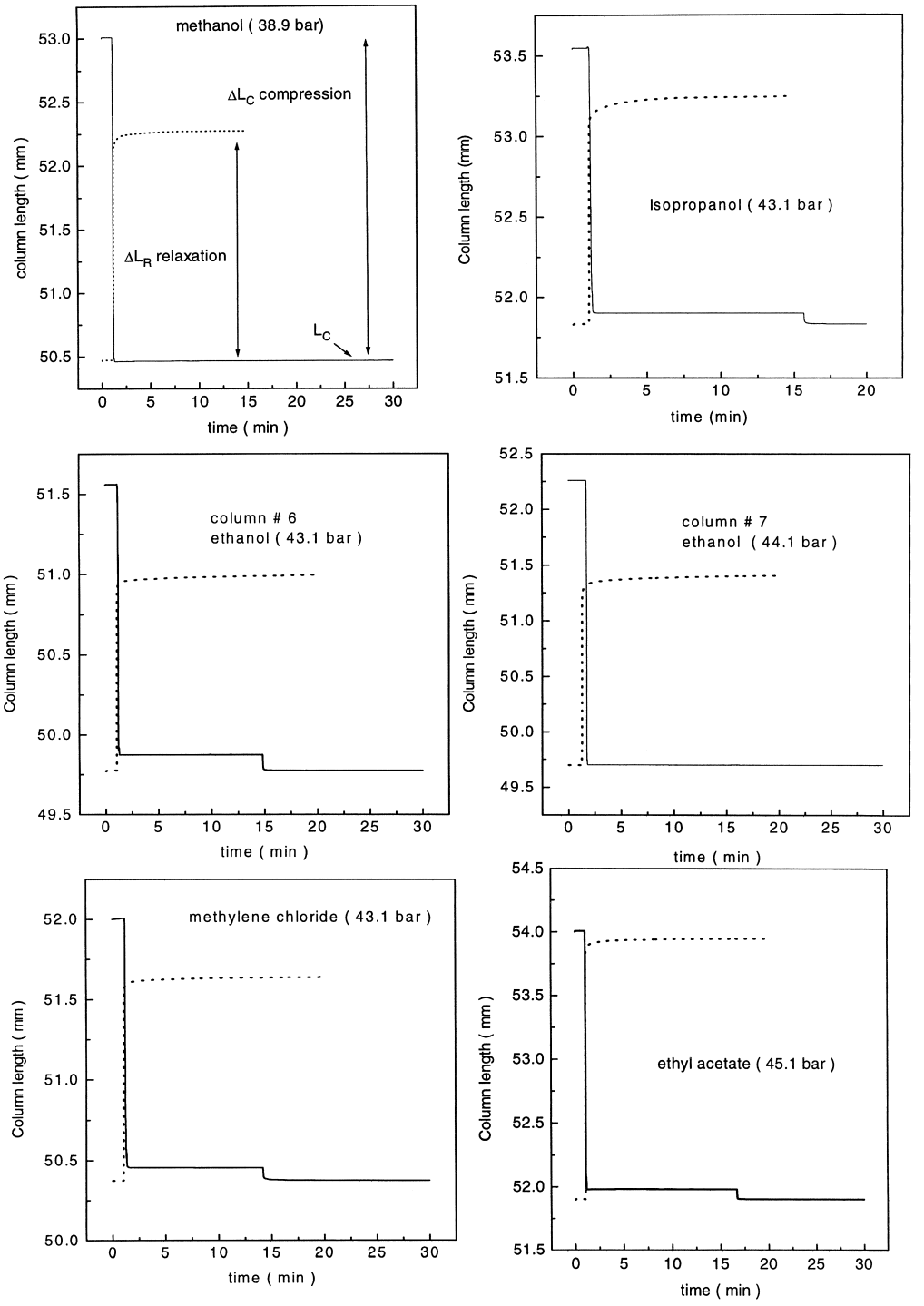

Fig. 2. Plot of the bed length versus time during the consolidation of columns packed in different slurry solvents; 60 g of Kromasil C_8 10 μm.

al used, the consolidation curves were all similar to the one obtained for the column packed with 60 g in methanol (see Fig. 2a). However, bed consolidation is an indefinite process that lasts forever [33,34]. The extent of consolidation achieved in a given time decreases rapidly with increasing time and, after half an hour, only long periods of time produce a measurable decrease of the bed length. Similar results were reported for columns packed with spherical particles whereas more frequent successive and random collapses occurred when irregular particles were used instead [11–18].

After completion of the first consolidation, the hydraulic jack that controls the movement of the piston (downward or upward) was abruptly released, leaving the piston free to slide backward, releasing the mechanical stress accumulated in the compressed bed. Fig. 2 also illustrates the change in bed length after this abrupt release of the compression stress. The bed expands rapidly but to a shorter extent than it had compressed initially ($\Delta L_R < \Delta L_C$, Fig. 2). For example, in methanol, the bed contracted by 5.3% of its initial length during consolidation and then expanded by only 3% during the relaxation step. The compression and relaxation data are reported in Table 1 for five columns, all packed in methanol under an axial stress of 40 bar. The change of bed length was always higher after compression than after relaxation. Conversely, the module of elasticity, *E*, was higher when the stress was released than when it was applied, a result that is classical in soil mechanics [33,34]. Consolidated columns behave more elastically after their first compression. The limited expansion of the column when stress is released is explained by the friction that takes place between particles and between the packed bed and the wall. Otherwise, the bed would return to its initial length, its length before the first compression stress had been applied. The relative change of bed length, whether in the compression or the relaxation mode, decreases with increasing amount of packing material (i.e., with increasing bed length). This has to do with the axial distribution of stress in the consolidated bed [35]. It is important to note that a second, or any further, compression of a previously consolidated bed does not cause a major change in the bed length, provided this new consolidation takes place under a stress not higher than the initial consolidation stress. This is also explained by the strong friction of the bed against the wall. Once consolidated, a particle bed behaves elastically when the compression stress is applied and released.

The measured or apparent elasticity modulus of the bed in the consolidation mode, E_c, almost doubles when the amount of packing material used increases from 30 to 240 g, as illustrated in Fig. 3. In the relaxation mode, the modulus, E_r, increases four times. This result indicates a large degree of heterogeneity of the mechanical stress, hence of the packing density of the bed along the column. It further indicates that this degree of heterogeneity increases with increasing bed length. The reason for that is a decrease of the extent of consolidation with increasing distance from the piston [35]. Previous experiments carried out with Zorbax C_{18} consolidated under similar compression stress showed the

Table 1
Bed compressibility data

Amount (g)	ACP (bar)	*L* (mm)	ΔL_C, mm (%)	ΔL_R, mm (%)	E_C (MN/m^2)	E_R (MN/m^2)	V_T (ml) at 40 bar	ε_T [b] at 40 bar	K_0 [c] ($cm^2 \cdot 10^{10}$) at 40 bar	Kozeny–Carman constant, *k*
30	43.0	26.6	1.4 (5.3)	0.8 (3.0)	88.8	136.5	29.8	0.571	3.69	193
60	38.9	50.5	2.5 (5.0)	1.8 (3.6)	81.5	110.8	60.1	0.600	5.05	196
120	41.0	105.9	3.6 (3.4)	1.9 (1.8)	124.6	225.9	127.7	0.620	6.41	192
180	41.0	159.7	5.3 (3.3)	1.8 (1.1)	127.5	355.2	194.6	0.616	6.78	174
240	41.0	202.0	5.0 (2.5)	1.5 (0.7)	169.1	546.0	254.3	0.643	6.66	234
Analytical [a] 250×4.6 mm	na	250.0	na	na	na	na	2.7	0.650	4.29	390

[a] Slurry packed column in methanol at 300 bar.
[b] Total porosity of the bed.
[c] Column permeability.

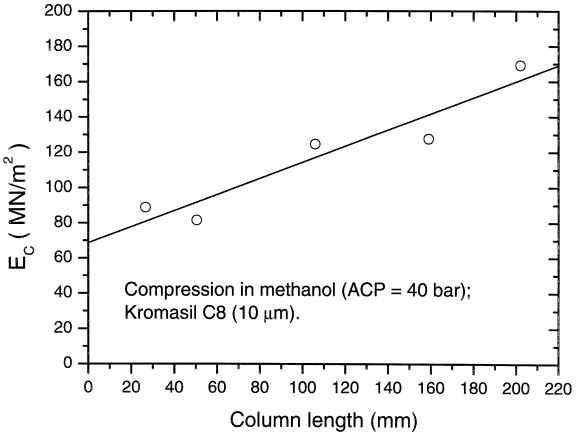

Fig. 3. Plot of the Young or elasticity modulus of beds packed with methanol as the slurry solvent versus the bed length (constant axial compression stress, 40 bar).

same behavior [19]. The increase of E with increasing bed length shows that the strain in the bed is not homogeneously distributed through the whole column, either radially or axially. It suggests that the stress is not homogeneous either, a result in agreement with the prediction of solid mechanics [35]. The amplitudes of the strain and stress distributions increase with increasing column length, explaining the difficulties encountered when trying to pack very long columns. These results are also consistent with those reported by Train in his study of the compression of powders into pellets [36]. Note, however, that the column length increases nearly in proportion to the mass of packing used (slope, 0.849 mm/g, intercept 1.65 mm, figure not shown, data in Table 1). This is consistent with the rather modest range of variations of the void ratio in the column.

3.2. Column permeability

The variation of the permeability with the column length confirms the presence of strain and stress gradients inside the column. The permeability of the columns packed in this study were derived from measurements of the inlet pressure of the column and of the corresponding flow-rate in the range 10–100 ml/min, using Darcy's law [37]. The values of the permeability for these columns are reported in Table 1. Note that the permeability obtained by this method is an average value, measured over the entire column. It would be difficult to measure the local permeability in different sections of the column.

The permeability, K_0, of a bed is related to the particle diameter, d_p, and to the external porosity, ε_e, of that bed by the combination of Darcy's law and the Kozeny–Carman equation [37], as follows:

$$K_0 = \frac{\epsilon_e^3 d_p^2}{\kappa(1-\epsilon_e)^2} \quad (1)$$

where κ is a constant, usually 180 for spherical particles. Since the volume of retention of thiourea was found to be nearly constant within the flow-rate range studied, the average total porosity of the bed was derived by averaging the values of the retention volume and subtracting the extra-column volume. Plots of the column permeability versus its length for compressed (axial stress, 40 bar) and relaxed beds (axial stress, 1 bar) are shown in Fig. 4. The permeability increases rapidly with increasing column length up to ca. 110 mm (corresponding to 120 g of packing material) and insignificantly for longer beds. The permeability of the column packed with 120 g is 74% higher than that of the column packed with 30 g and nearly the same as that of a twice

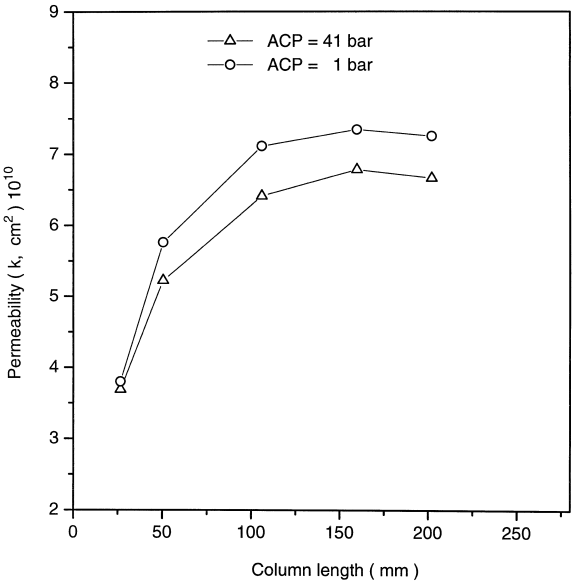

Fig. 4. Permeability of columns packed with methanol as the slurry solvent versus the bed length; solvent: methanol; axial compression stress: 41 bar and 1 bar (stress released).

longer column. Meanwhile, the corresponding total porosity increased by 8.6%. This result agrees with the variation of the permeability and the porosity of columns with their length as previously reported [15,18]. The same method was used to measure the permeability of the slurry packed analytical column, in the same range of mobile-phase linear velocity. Its permeability (Table 1) was larger than that of the shortest wide-bore column, packed with 30 g of material, but smaller than that of the column packed with 60 g. Its total porosity was higher than those of all the preparative columns (Table 1). Although a little particle breakage may have occurred during the preparation of this analytical column, this comparison shows that slurry packing provides a degree of consolidation comparable to that obtained with axial compression.

From experimental values of the bed porosity and permeability, it is easy to derive the Blake–Carman constant, κ. We assumed that the internal porosity of the packing material remains constant in all the experiments, the compression stress affecting exclusively the external porosity of the packed bed. This assumption is supported by previous results [15] demonstrating that the internal porosity of the packing material remains constant until major particle breakage takes place. The internal porosity of the packing material used was derived from measurements carried out on the analytical column, using the method of inverse size-exclusion chromatography previously described [38]. Samples of polystyrene of known molecular masses and narrow-molecular-mass distributions were injected on this column. Methylene chloride was used as the mobile phase (flow-rate = 1 ml/min) to ensure that these samples are not retained. The total porosity of the analytical column, derived from the retention time of toluene was 0.69, slightly higher than that derived from the retention volume of thiourea in methanol, 0.65. A slight adsorption of toluene could explain the small difference observed. A value of 0.37 was adopted for the external porosity of the analytical column. Finally, the plot of the logarithm of the retention volume of the polystyrene samples versus their molecular mass afforded the internal porosity of the packing material. This value was combined with the total porosity of the columns obtained by axial compression to determine their external porosity, from which the Blake–Carman constant was derived. The columns were assumed to be fully consolidated under a stress of 40 bar. The values obtained for the different columns are reported in Table 1.

Most of the values of the Blake–Carman constant obtained are in excellent agreement with the one usually recommended, 180, except for the analytical column. The longest column ($L = 20$ cm) and the analytical column gave larger values, corresponding to column permeabilities lower than predicted by the correlation. In general, however, Eq. (1) provides an excellent estimate of the permeability of a column, provided the porosities of the material used are available. It is possible but unlikely that the high value obtained for the longest column be due to particle breakage occurring during consolidation of the packing, as previously reported [13,17]. Finally, note in Fig. 4 that the plot of the permeabilities of columns consolidated under 41 bar versus their length is below the similar plot of the permeabilities measured in the relaxation mode. This result is explained by the expansion of the bed when the compression stress is released, hence by the increase of the external porosity of the column.

3.3. Effect of the nature of the slurry solvent on the kinetic of consolidation

Selecting the proper slurry and packing solvents for the preparation of a column is never simple. Several parameters may influence the final properties of the column and especially its eventual performance. This choice is one of them. A series of similar experiments were carried out on columns all filled with 60 g of packing material and all consolidated under an axial compression stress of approximately 40 bar. The difference between all these columns was the nature of the slurry solvent.

The plots of the bed length versus time following the rapid application of the axial stress (Fig. 2) showed a behavior similar to that reported for methanol. For all the columns studied, the consolidation was very rapid and smooth (not all the figures are shown). It is important to note that water did not wet the stationary phase, the particles of which could not be dispersed in this solvent, making it impossible to prepare a slurry and fill the column with it. In order to study the consolidation in water, the par-

ticles were first suspended in methanol and the slurry was immediately poured into the column. The top of the column was closed and the piston raised until the compression pressure reached 2 bar. The column was left quiet for few minutes, then the axial compression stress was released and the column was flushed with a few liters of water, to wash off the methanol contained in the porous particles of the stationary phase, the pump was stopped, and the compression stress was rapidly raised to 41 bar. During this experiment, the variation of the bed length versus time was similar to that observed in the other cases. The bed behaved elastically when the compression stress was applied or released (figure not shown). No significant variation of the bed length was observed when operating any of these columns for several days under constant compression stress.

The compressibility data measures for all the columns studied are given in Table 2. The results show that the decrease of the bed length, ΔL_C for the first compression is larger than the bed expansion upon relaxation, ΔL_R. The column packed in methanol and consolidated under a stress of 38.9 bar exhibits the largest relative decrease of bed length upon compression (5%) and the greatest relative increase upon relaxation (3.6%). This result suggests that the bed packed in methanol experiences the smallest degree of friction against the wall of the column cylinder under the selected experimental conditions (external axial stress, 40 bar). Other results regarding this column were discussed earlier (see Table 1, and Figs. 2a, 3, and 4). The columns 3, 4, 6 and 7 in Table 2, were packed in *n*-hexane, *n*-octanol and ethanol, respectively. They exhibited the same behavior, attributed to friction between the bed and the wall. The compressibility data suggest also that the intensity of the wall effect increases with increasing compression stress, hence with the extent of consolidation.

The permeability and the porosity of most col-

Table 2
Compressibility data[a]

No.	Slurry solvent	η (cP)	ACP (bar)	L (mm)	ΔL_C, mm (%)	ΔL_R, mm (%)	E_C (MN/m^2)	E_R (MN/m^2)	V_T[b] (ml)	ε_T	K_0 (cm^2 ·10^{10})	Kozeny–Carman constant, k
1	Methanol	0.60	11.3	54.3	0.7 (1.3)	0.4 (0.7)	91.1	158.1	na	na	na	
1	Methanol	0.60	21.1	53.0	1.3 (2.4)	0.9 (1.7)	85.6	117.7	na	na	na	
1	Methanol	0.60	38.9	50.5	2.5 (5.0)	1.8 (3.6)	81.5	110.8	60.1 (a)	0.600	5.05	196
2	Isopropanol	2.40	43.1	51.8	1.7 (3.3)	1.4 (2.7)	134.6	157.9	61.3	0.618	5.49	219
3	*n*-Hexane	0.32	21.5	53.1	0.9 (1.7)	0.7 (1.3)	118.9	165.8	na	na	na	
3	*n*-Hexane	0.32	45.1	51.5	2.2 (4.3)	1.6 (3.1)	109.9	147.5	65.5 (b)	0.654	4.72	369
4	*n*-Octanol	0.32	20.5	52.0	1.0 (1.9)	0.7 (1.3)	108.9	149.7	na	na	na	
4	*n*-Octanol	9.12	43.1	49.6	2.2 (4.4)	1.6 (3.2)	102.0	133.2	63.3 (b)	0.645	7.12	224
5	Acetonitrile	0.37	45.1	50.8	1.9 (3.7)	1.5 (3.0)	121.7	153.9	59.9	0.601	4.98	201
6	Ethanol	0.37	20.5	51.0	0.9 (1.8)	0.5 (1.0)	112.4	208.9	na	na	na	
6	Ethanol	1.20	43.1	50.8	1.8 (3.5)	1.5 (3.0)	124.9	175.7	60.9	0.607	4.28	253
7	Ethanol	1.20	20.5	51.6	1.4 (2.7)	0.7 (1.4)	76.4	208.9	na	na	na	
7	Ethanol	1.20	44.1	49.7	2.5 (5.0)	1.7 (3.4)	90.0	128.4	61.4	0.608	4.34	
7	Methanol*	0.60	41.1	51.0	na	1.5 (2.9)	na	141.6	61.7	0.610	5.22	
8	Ethylene glycol	19.90	41.0	50.7	2.3 (4.5)	1.7 (3.4)	94.5	121.1	59.8	0.609	10.06	
9	Ethylene glycol	19.90	41.0	50.9	2.1 (4.2)	1.6 (3.1)	102.2	133.0	60.1	0.595	9.25	101
9	Methanol**	0.60	41.0	50.9	na	na	na	na	60.6	0.600	5.09	
10	Water	1.00	41.0	52.3	1.7 (3.3)	1.3 (2.6)	132.0	165.1	36.0	0.353	5.99	497
11	Acetone	0.32	43.1	50.6	2.4 (4.7)	1.9 (3.8)	95.8	112.2	68.4	0.657	4.76	377
12	Methylene chloride	0.44	43.1	50.4	1.6 (3.2)	1.3 (2.6)	137.8	171.4	65.2 (b)	0.664	5.87	327
13	Ethyl acetate	0.45	45.1	50.4	2.1 (4.2)	2.0 (4.0)	116.2	114.5	70.0	0.702	5.33	518

[a] A 60-g amount of Kromasil C_8 in 200 ml of solvent.

[b] V_T: Measured by injecting thiourea.

* & **: Columns consolidated in ethanol and ethylene glycol under 41 bar, respectively. ΔL_C and ΔL_R: variation of length for compressed and relaxed columns, respectively. E_C and E_R: module of elasticity for compressed and relaxed bed, respectively. Total porosity, ε_T at 40 bar; permeability, K_0.

umns were measured under the highest compression stress. The results are also given in Table 2. The lowest permeability was measured for column 6, packed in ethanol, the highest permeability for columns 8 and 9, packed in ethylene glycol, and the second highest for column 4, packed in *n*-octanol. Overall, the permeability appears to increase, hence the bed packing density to decrease with increasing viscosity of the packing solvent. Only small differences of permeability are observed between columns 1, 7, and 9, packed under the same experimental conditions with methanol or between columns 6 and 7, packed with ethanol. This illustrates the good reproducibility of the packing procedure. The graphs in Fig. 5 show the variation of the bed length (top line) and the inlet pressure (bottom line) of the liquid flowing through the column maintained under a compression stress of 40 bar during a change of the solvent percolating through the column, from ethanol (top graph) or ethylene glycol (bottom graph) to methanol. No significant variation of the bed length was observed during this experiment. Replacing ethanol or ethylene glycol by methanol did not appear to affect the morphology of the bed as long as the compression stress was maintained. Meanwhile, the inlet pressure of the liquid increased rapidly when the pump was started, then decreased rapidly and smoothly. After several volumes of methanol had percolated through the column, the stress was released, letting the packing bed free to bounce back. The increase of the bed length was similar to that observed for the column consolidated in the original solvent.

The column consolidated in water exhibits by far the lowest total porosity, 0.353 (but not a permeability much different from the average permeability of the 13 columns prepared). This porosity is abnormally low. It is close to (but slightly lower than) the external porosity of the analytical column measured by inverse size-exclusion chromatography, using methylene chloride as the mobile phase and a series of polystyrene standards as the molecular probe (0.37, see earlier). This result is almost certainly explained by water not wetting the stationary phase. Several injections of a thiourea solution were carried out on the analytical column using water as the mobile phase. The retention volume was found nearly constant in the flow-rate range from 0.1 to 1

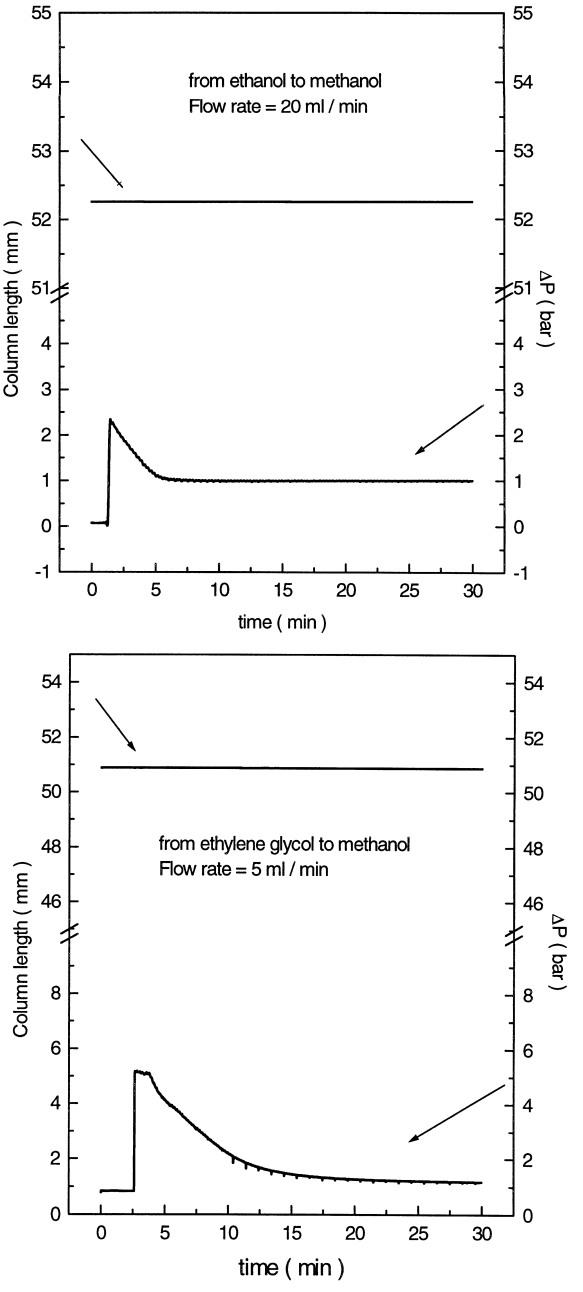

Fig. 5. Change in the bed length and pressure drop upon replacement of the slurry solvent (top, ethanol; bottom, ethylene glycol) by methanol; 60 g of Kromasil C_8 (10 μm).

ml/min, showing that there was no significant change of the wet area of the packing material with increasing inlet pressure of water in the corre-

sponding pressure range (1 to 100 atm). The average values of the retention volume and the column porosity were 1.67 ml and 0.405, respectively. This value of the porosity is nearly the same as the external porosity derived by size-exclusion chromatography, 0.37. This suggests that thiourea cannot access the internal volume of the stationary phase when water is used as the mobile phase. One could probably make a quick estimate of the external porosity of a reversed-phase chromatography column by using water as the mobile phase, injecting thiourea, and deriving its retention volume. However, this property may not be the same for all RPLC materials.

3.4. Effect of the nature of the slurry solvent on the column efficiency

Figs. 6 and 7 illustrate the variation of the reduced plate height versus the reduced flow velocity for columns packed with 240 g of Kromasil C_8, with different slurry solvents, and consolidated under 40 bar. The efficiencies of the two compounds were measured in the same range of linear velocity. Thus, the higher values of the reduced velocity in the $h(v)$ plots for PTD are explained by its approximately three times lower diffusion coefficient [31]. Note that all the values of h were corrected for the extra-column variance contribution (see Experimental).

All the plots of the reduced HETP versus the reduced velocity follow a typical Van Deemter equation [32] behavior. They exhibit a minimum of the reduced HETP for a reduced velocity of ca. 2 for thiourea or ca. 6.5 for PTD. At higher reduced velocities, the reduced HETP varies only slightly if at all, illustrating the fast mass transfer of the two compounds studied. The experimental data were fitted to the following equation:

$$h = a + \frac{b}{v} + cv \qquad (2)$$

where a, b, and c are numerical coefficients. The contribution of interest in this work is that of Eddy diffusion, a. Poor bed uniformity results in flow channeling and in pathway heterogeneity, spreading the solute band. The other two contributions, due to axial diffusion of the band (b) and to the mass transfer resistances (c) are not affected by the degree

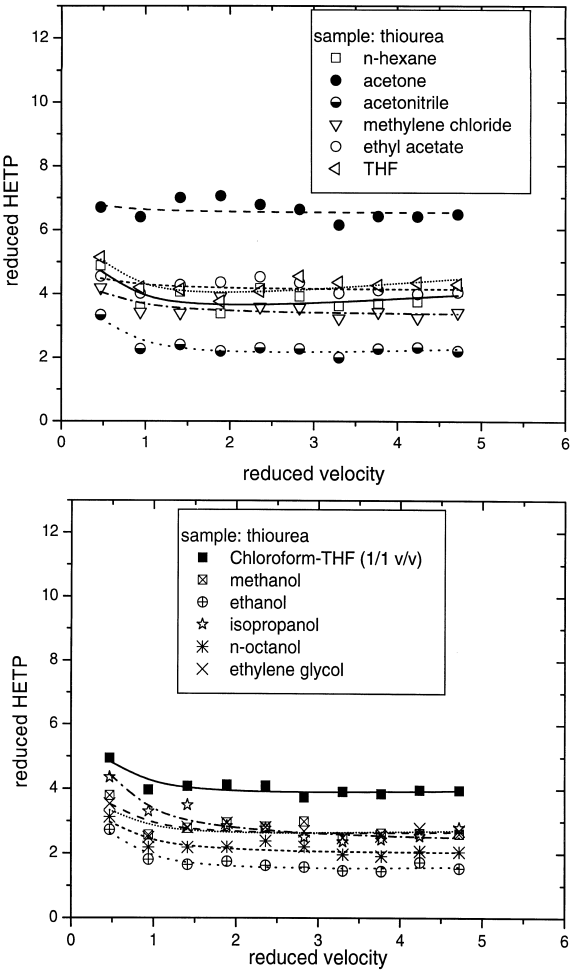

Fig. 6. Plots of the reduced plate height versus the reduced velocity for columns consolidated with different slurry solvents; 240 g of Kromasil C_8; mobile phase: methanol; sample: thiourea.

of heterogeneity of the bed, at least in a first approximation, Eq. (2). The estimates of the parameters a, b and c derived from measurements made on columns packed with 240 g in several solvents are illustrated in Table 3. Values of the reduced HETP, h, at the reduced velocity corresponding to a linear velocity $u = 3.3$, of the column length, its total porosity (derived from the retention time of thiourea unretained), and its permeability (for a methanol stream) are also reported in this table.

The nature of the slurry solvent does not influence significantly the total porosity. The values obtained with the different slurry solvents are between 0.626

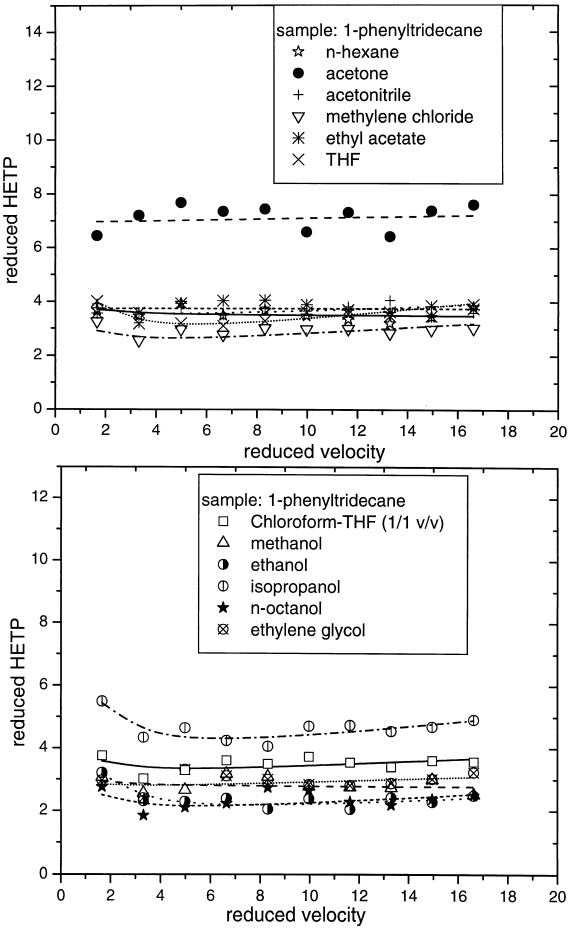

Fig. 7. Plots of the reduced plate height versus the reduced velocity for columns consolidated with different slurry solvents; 240 g of Kromasil C_8; mobile phase: methanol; sample: 1-phenyltridecane.

and 0.642, a narrow range, and we consider the relative standard deviation (RSD) of ca. 0.7% as not significant. The RSD of ca. 0.7% for the bed length measured with the various slurry solvents is also not important a this stage. These figures illustrate the very good overall reproducibility of the packing procedure. By contrast, the column permeabilities depend markedly on the nature of the slurry solvent (RSD = ca. 5.1%), which indicates a significant influence latter on the texture and/or morphology of the bed obtained.

A low permeability and/or a high packing density do not necessarily lead to a high column efficiency. Surprisingly, the highest values of the HETP for both samples were obtained with the column packed with acetone as the slurry solvent. This column has the lowest permeability (Table 3) and the worst efficiency (reduced HETP of ca. 6 and 7 for thiourea and PTD, Figs. 6 and 7). It also exhibits the highest a (ca. 6.502) value for thiourea, indicating that it has the most heterogeneous bed. *n*-Hexane seemed to be a much better slurry solvent than acetone, even though both solvents have the same viscosity. This could be explained by a better dispersion of silica C_8 particles in *n*-hexane, due to the similarity of the solvent molecule and the bonded ligand.

An important improvement in the column quality was observed when the viscosity of the slurry solvent was increased and/or its chemical structure was closer to that of the ligand. Thus, *n*-octanol gave nearly the lowest HETP for both samples. It is likely that the hydroxyl group of *n*-octanol interacts with the residual silanol groups on the surface of the packing material while the alkyl chains of solvent and RPLC packing also interact. This would cause a better wetting of the stationary phase by the slurry solvent. Note that, from *n*-hexane to 1-octanol, the value of the a parameter drops from 2.8 to 1.8 and the reduced HETP from 3.6 to 2.0 for thiourea. A similar behavior was observed for PTD. Unfortunately, these two slurry solvents are immiscible with water and most methanol–water mixtures, solvents commonly used as the mobile phase in RPLC. Replacing the slurry solvent by the mobile phase required washing the column with an intermediate solvent that is miscible with both the mobile phase and the slurry solvent. This is an expensive proposition that could be justified only if a major improvement in the column efficiency could be reliably achieved. Our results (Table 3) suggest such an improvement but do not yet demonstrate it entirely. In the mean time, packing columns with a slurry solvent miscible with methanol–water mixtures remains more economical in preparative HPLC because solvent costs are an important factor.

Acetonitrile is a better alternative since the column exhibits a very good performance (ca. $a = 1.622$ and HETP = 2.00 for thiourea). Columns packed with methylene chloride, ethyl acetate (both immiscible with water), and THF exhibited only a fair efficiency. No efficiency improvement was observed

Table 3
Reduced parameters of the Van Deemter equation[a]

Slurry solvent	η (cP)	L (cm)	ε_T	K ($cm^2 \cdot 10^{-10}$)	Thiourea ($D_0 = 1.8 \cdot 10^{-5}$ cm^2/s)			1-Phenyltridecane ($D_0 = 0.51 \cdot 10^{-5}$ cm^2/s)			
					a (RSD, %)	b (RSD, %)	h ($u = 3.3$)	k'	a	b	h ($u = 3.3$)
n-Hexane	0.32	20.95	0.638	6.97	3.610 (4.6)	0.409 (54.7)	3.62	1.18	3.456 (3.0)	0.420 (106.7)	3.46
Acetone	0.32	20.75	0.631	6.30	6.502 (2.1)	0.122 (137.4)	6.14	1.22	7.092 (3.5)	0.000	7.21
Acetonitrile	0.37	20.95	0.630	6.57	2.034 (4.0)	0.483 (25.8)	2.00	1.20	3.686 (3.6)	0.000	3.20
Methylene chloride	0.44	21.15	0.638	7.15	3.296 (3.0)	0.361 (36.3)	3.59	1.16	2.889 (3.4)	0.170 (252.8)	2.65
Ethyl acetate	0.45	21.05	0.637	7.14	4.097 (2.3)	0.183 (63.9)	4.02	1.19	3.739 (2.7)	0.000	3.58
THF	0.51	21.10	0.634	7.15	4.063 (3.6)	0.347 (55.5)	4.36	1.17	3.418 (4.9)	0.255 (293.4)	3.17
Chloroform–THF (50:50, v/v)	0.59*	20.95	0.642	7.19	3.764 (2.0)	0.468 (22.1)	3.92	1.17	3.476 (3.5)	0.000	3.31
Methanol	0.60	21.25	0.633	7.03	2.517 (4.5)	0.443 (35.9)	2.40	1.22	2.750 (4.1)	0.301 (165.7)	2.56
Ethanol	1.20	20.85	0.628	6.33	1.382 (	0.539 (17.5)	1.47	1.25	2.114 (4.9)	1.370 (37.8)	2.43
Isopropanol	2.40	20.90	0.626	6.37	2.284 (4.6)	1.018 (16.3)	2.37	1.21	4.393 (4.0)	1.145 (71.2)	4.34
n-Octanol	9.12	21.05	0.633	7.04	1.911 (3.9)	0.485 (22.6)	1.97	1.17	2.296 (6.9)	0.000	1.85
Ethylene glycol	19.90	20.95	0.631	6.90	2.547 (4.1)	0.333 (43.0)	2.49	1.21	2.913 (4.8)	0.000	2.90
RSD (%)		0.7	0.7	5.1				2.3			

[a] A 240-g amount of Kromasil C_8 (10 μm); ACP stress = 40 bar; *, estimated value.

for the column packed with chloroform–THF (50:50, v/v), the characteristics of which are close to those obtained with THF. The results obtained with methanol are satisfactory, better than with acetonitrile for thiourea, worse for PTD (Table 3). The best efficiency for thiourea was obtained when the column was consolidated in ethanol, for PTD when in *n*-octanol. It could seem that increasing the viscosity of the slurry solvent from 0.6 (methanol) to 1.2 cP (ethanol) would lead to a decrease of the HETP. This explains the experiments made with isopropanol, *n*-octanol, and ethylene glycol. The column efficiency achieved was poor with isopropanol, better for PTD with glycol (in fact comparable to those with methanol), and excellent for both compounds with *n*-octanol.

A high viscosity of the slurry solvent is not sufficient for the packing of good columns. Selecting a slurry solvent having chemical properties similar to those of the packing material is also an important requirement. The total porosity of columns packed in *n*-octanol and in isopropanol are similar (difference 0.7%), but the permeability of the former column is 7.1% higher than that of the latter while its HETP and a parameter for PTD much smaller. This result also shows that a column with a higher permeability can both be more homogeneous and exhibit a better performance (Table 3).

Finally, it should be noted that the mass transfer term is small in all cases and has little influence on the band broadening. This was expected, given the choice of the samples and the independence between the mass transfer kinetics and the homogeneity of the column bed.

3.5. Friction measurements

All these measurements were carried out on columns consolidated under 40 bar for several hours. The experimental design is illustrated in Fig. 1 and discussed in the Experimental section. A first measurement of the friction shear stress was performed without packing material, to determine the blank [19]. The inlet pressure of methanol and the displacement of the piston observed in this case are plotted versus time in Fig. 8 (top graph). The piston started moving at a constant velocity when the pressure reached an approximate value of 3 bar. Then, the methanol pressure dropped rapidly and remained constant with no significant variation after a short (ca. 1 min) period of stabilization. This effect arises from the dynamic sliding friction shear of the

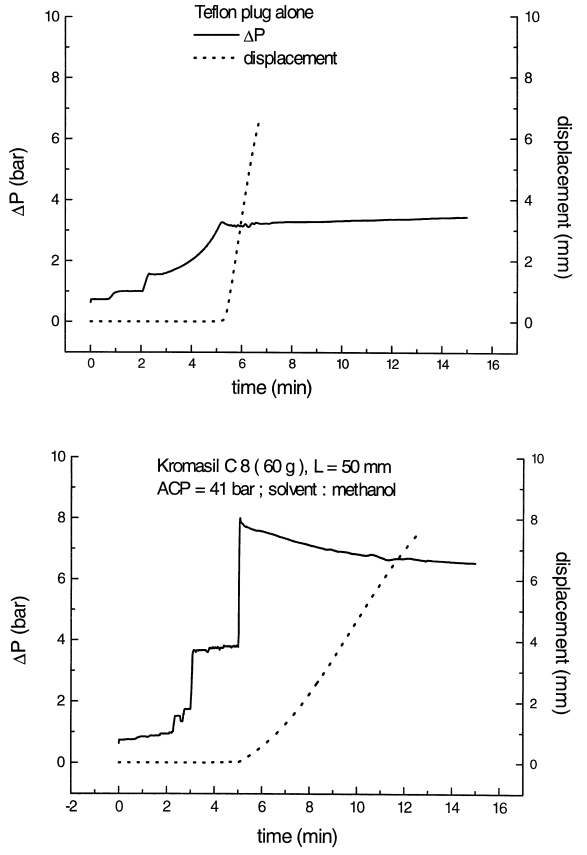

Fig. 8. Measurements of the friction of the PTFE plug in an empty column (top) and a column packed with methanol as the slurry solvent.

bed against the wall being constant and lower than the static friction shear that needs to be overcome by the pressure stress acting on the plug before the sliding motion can begin. The PTFE plug kept sliding at a constant velocity (Fig. 8). Note that, because of the limited range of the position sensor, displacements in excess of 7.5 mm could not be recorded.

Similar experiments were carried out on columns packed with slurries made with 60 g of Kromasil C_8 in different solvents and consolidated under an axial stress of 40 bar for at least 2 h, in order to ensure full consolidation (see earlier discussion and Fig. 2). The axial stress was first released, causing a slight expansion of the bed (see earlier). Then, methanol was pumped above the PTFE plug. Fig. 8 (bottom graph) shows typical plots of the pressure of methanol and of the position of the piston versus time for a bed packed from a methanol slurry. No movement was observed until the pressure reached 8 bar. Then, the pressure decreased rapidly and reached a steady state while the bed moved at a nearly constant velocity.

Plots of the pressure above the PTFE plug versus time for columns packed with other slurry solvents are shown in Fig. 9. These curves present two maxima, in contrast with the one corresponding to the column consolidated in methanol for which a rapid increase of the pressure above the PTFE plug is followed by a smooth decrease during the shear stress measurement (Fig. 8). The column packed with the methanol slurry also exhibited the lowest pressure excursion, hence the lowest friction shear stress. For most other columns, the pressure dropped when the bed started slipping (first maximum) but a second pressure maximum was observed before steady state was reached. The intensity of this phenomenon appears to be related to the importance of the friction shear stress. It could be explained by a secondary consolidation of the bed. In all experiments so far, the bed is consolidated by the upward movement of the piston (Fig. 1) and the packing density of the consolidated bed decreases from the bottom of the column upward. In the experiment discussed, the bed is pushed out of the column in the downward direction. If the axial stress applied to the column top by the plug exceeds the consolidation stress applied there during the initial stage, further consolidation will take place. This explains the increase of the friction shear between the bed and the wall. It could also cause particle breakage to a certain extent.

The values of the maximum (or two maxima) static shear stress and of the dynamic shear stress obtained for the different columns are reported in Table 4 as the corresponding methanol pressure. These values are corrected for the blank, i.e., the contribution of the friction shear of the PTFE plug against the wall (which is why the values seen in Fig. 9 are ca. 3 bar higher than those in Table 4). Table 4 also reports the RSDs of the maximum values of the stress needed to force the bed to slide, values derived from multiplicate measurements. Most of these RSDs are below 8% and none exceed 13%. As

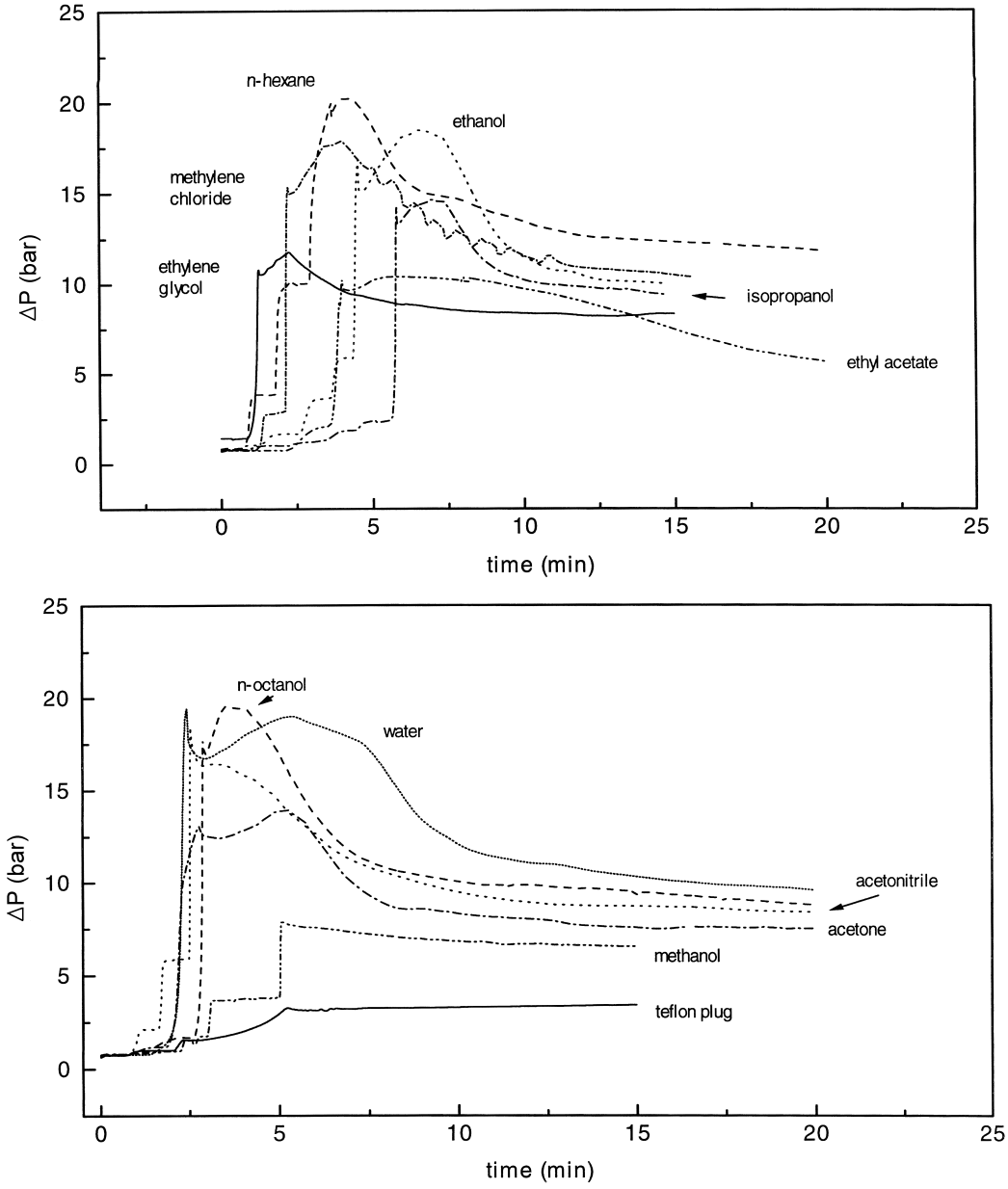

Fig. 9. Effect of the nature of the slurry solvent on the bed–wall friction; 60 g of Kromasil C_8 (10 μm); compression stress: 40 bar.

explained above, the column packed with methanol exhibits the lowest average shear stress. The highest average value was obtained for the column packed with *n*-hexane, with water a close second. The value obtained for isopropanol, often recommended as the packing and slurry solvent, is much larger than that for methanol. No correlation exists between these friction shear stresses and the viscosity of the slurry solvent (Table 4).

Independent measurements showed that the friction coefficients of thin, consolidated beds of Kromasil C_8 or of Zorbax C_{18} against a stainless

Table 4
Corrected values of shear stress obtained for columns packed with 60 g of Kromasil C_8 and consolidated under 40 bar

Solvent	η (cP)	Polarity index [1]	First maximum ΔP (bar)	Second maximum ΔP (bar)	Average ΔP (bar)	RSD (%)
Methanol	0.60	5.1	4.7	#	4.7	#
Ethyl acetate	0.45	4.4	6.9	7.1	7.0	2.0
Ethylene glycol	19.90	na	7.5	8.5	8.0	8.8
Acetone	0.32	5.1	9.8	10.7	10.3	6.2
Isopropanol	2.40	3.9	10.9	11.3	11.1	2.5
Methylene chloride	0.44	3.1	12.1	14.5	13.3	12.8
Ethanol	1.20	5.2	13.5	15.1	14.3	7.9
n-Octanol	9.12	na	14.5	16.2	15.4	7.8
Acetonitrile	0.37	5.8	15.1	15.7	15.4	1.8
Water	1.00	10.2	16.1	15.7	15.9	1.8
n-Hexane	0.32	0.1	16.7	16.9	16.8	0.8
PTFE plug	#		3.3	#	#	#

steel plate are independent of the nature of the slurry solvent. Since the stress needed to force a sledge to skip is proportional to the friction coefficient and to its mass, the conclusion of these seemingly contradictory results is that the radial stress applied by a bed consolidated under axial compression stress against the column wall is a function of the nature of the slurry solvent. This radial or transverse stress depends on the particle–particle [40] and the particle–wall [39] frictions. It also depends on the interactions of the external surface of the particles and the wall with the solvent, interactions that are affected by adsorption of this solvent on the solid surfaces involved, hence on the nature of the solvent. It is even likely that the actual surface areas of contact between the bed and the wall and between particles vary from one solvent to another. It is nevertheless striking that the friction shear stress derived from measurements carried out on columns packed using *n*-hexane, *n*-octanol, acetonitrile, and water as the slurry solvent are very close, even though the former three solvents wet well the particles of Kromasil C_8 while water does not.

3.6. Influence of the bed length on the friction shear stress

Similar experiments were carried out with beds of different lengths, packed with increasingly large amounts of material, always using methanol as the slurry solvent, and all consolidated under 40 bar for at least 2 h. The slurry concentration also was kept constant for all columns and fresh packing material was used for the preparation of each column. Fig. 10 shows the variation of the shear stress at the column wall, measured as the methanol pressure applied above the 5 cm I.D. PTFE plug, versus the time. Data are reported for columns packed with 30, 60, 120, 180, and 240 g of Kromasil C_8. A similar

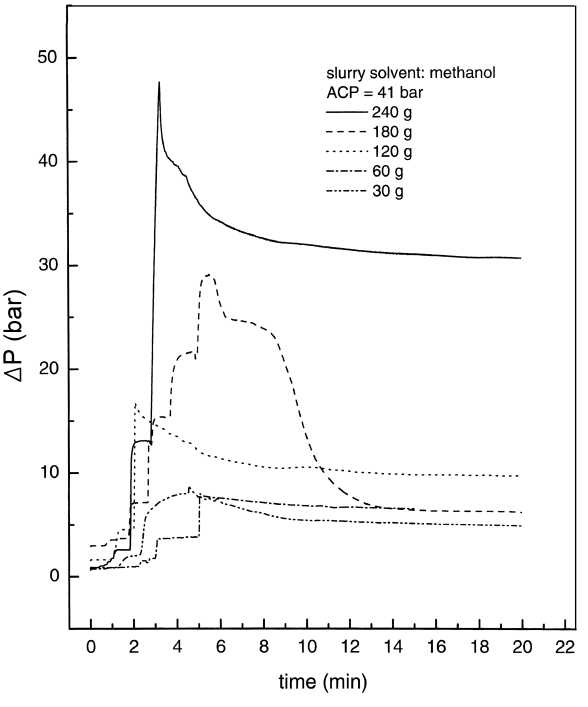

Fig. 10. Effect of the bed length on the bed–wall friction; slurry solvent: methanol; compression stress: 40 bar.

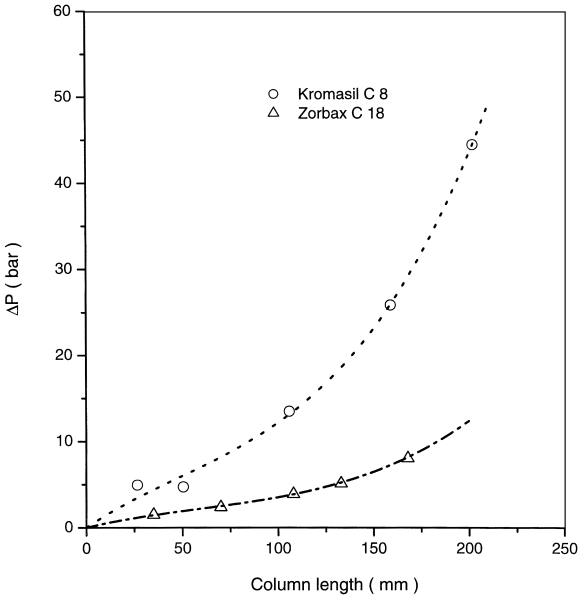

Fig. 11. Shear plot of the bed–wall stress versus the bed length.

behavior was observed for all columns. When methanol is pumped, the pressure above the plug increases progressively while the bed remains steady until it reaches the value of the shear stress. Then, it decreases rapidly and the bed begins to slide at a constant velocity, proportional to the pump flow-rate. Some intermediate steps were observed when the methanol pressure was stopped to check how stable was the bed–wall junction under shear stress.

A plot of the constant pressure measured during the dynamic or steady-state sliding of the bed versus its length is shown in Fig. 11. This plot is compared with the one derived from a previous study, carried out on columns packed with Zorbax C_{18}, with methanol as the slurry solvent, and consolidated under 40 bar [19]. The values of the static threshold and the dynamic shear stresses are reported in Table 5. The values measured for the columns packed with 30 and 60 g seem close. This might be a fluke due to some experimental errors because, for the other columns the shear stress increases rapidly with increasing bed length and/or packing amount, especially above 120 g of Kromasil C_8. A similar trend but one of considerably less amplitude was observed for the columns packed with Zorbax C_{18}. In a large part, this difference should be ascribed to the differences between the shape of the particles (see photographs in Refs. [13,40]) since the effect of the internal friction angle of the two materials [40] would suggest the opposite result. The values measured for this angle are 26° and 40° for stationary phases very similar to Kromasil and Zorbax, respectively [40]. Therefore, another important question raised by our work is why is the friction shear stress higher with the material that flows better?

We are confronting here a fundamental issue that is not yet settled: what controls the friction of a particulate material against the wall of its container? Tribology [41–44], the science of friction, has remained until quite recently most empirical, an art more dedicated to the propagation of technical tales of dubious validity and uncertain origin than a science dedicated to the understanding of physical phenomena through fundamental investigations [41]. Fundamental studies of friction undertaken at the molecular level have debunked several legends, among them the concept that friction was more intense against ruguous surfaces than against smooth ones [41]. Scientists still do not know how lubricants lubricate [43]. What seems highly probable now,

Table 5
Compressibility data for columns consolidated in methanol

Amount (g)	$-dL/dP$ (cm^3/MN)	L_0 [a] (mm)	a_v [b] (cm^2/MN)	e_0 [a]	E (MN/m^2)	k_0 [a] (cm^2)	$-dk/dP$ (cm^2/bar)
60	729	54.3	173.5	0.6652	96.3	$6.33\cdot10^{-10}$	$3.02\cdot10^{-12}$
120 (first compression)	774	103.3	126.6	0.6906	133.5	$6.73\cdot10^{-10}$	$1.78\cdot10^{-12}$
120 (second compression)	523	101.4	85.7	0.6613	193.9	$5.92\cdot10^{-10}$	$1.34\cdot10^{-12}$

[a] L_0, e_0 and k_0, column length, void ratio and permeability at zero pressure, respectively.

[b] $a_v = -\frac{de}{dP}$: compressibility coefficient.

however, is that friction can be and often is reduced by spatial disorder and/or thermal noise [44]. This would explains our observations.

The column wall is smooth at the scale of the particle size (wall asperities are ca. 100 times smaller than the average particle diameter). For this reason, the first layer of particles forms a less irregular, slightly more ordered layer against the wall. This layer anchors a second layer and making it slip against the wall is difficult, hence the high friction shear stress. This stress is higher for the more regular Kromasil, the particles of which are, in their immense majority, nicely spherical than for the lesser regular Zorbax, the particles of which are, in a significant fraction ''siamese twins'' or even ''siamese triplets'' [13,40]. A lower degree of order of the particles in their first layer against the column wall would explain the results illustrated in Fig. 11. Whether it is possible to combine the results of our study and applications of the new concepts generated by recent fundamental research in tribology [41–44] to the preparation of more efficient columns is under investigation.

4. Conclusion

This study documents the strong influence of the slurry solvent on the dynamics of consolidation of columns packed under axial compression. The compressibility data reported demonstrate clearly the importance of the wall effect during the preparation of chromatographic columns. The bed of a consolidated column expands rapidly, to an extent that depends on the shear stress at the column wall, when the axial compression stress is released. The column bed is radially heterogeneous.

The modulus of elasticity of the bed decreases with increasing axial compression stress, even after relaxation of this stress, because of the consolidation of the bed. The modulus increases with increasing bed length because the friction between the bed and the wall increases also with increasing bed length. Our results show also that the packing density varies along the column axis and that all column properties (e.g., its porosity, its permeability, the retention factors of probes, and the HETP) vary along the bed length. Thus, column beds are not homogeneous, either axially or radially. The column permeability and its porosity increase from the end where the axial compression stress is higher to the other end, so much so that friction is the major limiting factor for the packing of very long columns. A short column, however, one for which the length is close to or shorter than the diameter, could be much less heterogeneous than a column with a large aspect ratio. Although the efficiency of such a column should be excellent, the practical advantages would be nullified by the importance of the extra-column contribution to band broadening.

While the results summarized above are easily understood, two more observations remain puzzling. First, the porosity and the permeability of a column vary substantially from one slurry solvent to another. The lowest permeability was obtained for the column packed with ethanol while the column packed with a chloroform–THF (50:50, v/v) solution showed the highest permeability. Ethanol appeared the best choice as the slurry solvent because the corresponding column exhibits the best performance while the miscibility of this solution with common solvents used as the stationary phase in high-performance liquid chromatography and its moderate viscosity allow a very rapid change of the mobile phase. Also, the shear stress measured by forcing the bed to slip along the column wall depends much on the nature of the slurry solvent. The stress between the particles in the packed bed is conveyed to the wall to an extent that depends on the nature of the solvent because of the complex interactions involving adsorption of the solvent on the particles. Second, the friction shear stress of the bed along the column wall depends strongly on the nature of the packing material and, as a result, the material having the most regular, spherical particles is not necessarily the one affording the highest efficiency. Systematic investigations of this mechanical property of packing materials should be pursued.

Acknowledgements

This work was supported in part by grant DE-FG05-88-ER13869 of the US Department of Energy and by the cooperative agreement between the University of Tennessee and the Oak Ridge National

Laboratory. We acknowledge the loan of the LC.50.VE.500.100 column skid by Prochrom (Champigneulles, France) and the generous gift of Kromasil packing material by Akzo Nobel/Eka Chemicals. We thank Jacqueline Krim (North Carolina State University, Raleigh, NC, USA) for fruitful discussions.

References

[1] L.R. Snyder, J.J. Kirkland, J.L. Glajch, Practical HPLC Method Development, 2nd ed., Wiley, New York, 1997.
[2] G. Guiochon, S.G. Shirazi, A.M. Katti, Fundamentals of Preparative and Nonlinear Chromatography, Academic Press, Boston, MA, 1994.
[3] K. Mihlbachler, J. Fricke, T. Yun, A. Seidel-Morgenstern, H. Schmidt-Traub, G. Guiochon, J. Chromatogr. A 908 (2001) 49.
[4] K. Mihlbachler, A. Seidel-Morgenstern, G. Guiochon, manuscript in preparation.
[5] K.K. Unger, in: Porous Silica – Its Properties and Use as Support in Column Liquid Chromatography, Journal of Chromatography Library, Vol. 16, Elsevier, Amsterdam, 1979, p. 169.
[6] J. Klawiter, M. Kaminski, J.S. Kowalczyk, J. Chromatogr. 243 (1982) 207.
[7] M. Kaminski, J. Klawiter, J.S. Kowalczyk, J. Chromatogr. 243 (1982) 225.
[8] K. Prusiewicz, M. Kaminski, J. Klawiter, J. Chromatogr. 243 (1982) 232.
[9] M. Kaminski, J. Chromatogr. 589 (1992) 61.
[10] M. Sarker, G. Guiochon, J. Chromatogr. A 702 (1995) 27.
[11] G. Guiochon, M. Sarker, J. Chromatogr. A 704 (1995) 247.
[12] M. Sarker, G. Guiochon, J. Chromatogr. A 709 (1995) 227.
[13] M. Sarker, A.M. Katti, G. Guiochon, J. Chromatogr. A 719 (1996) 275.
[14] M. Sarker, G. Guiochon, J. Chromatogr. A 741 (1996) 165.
[15] B.J. Stanley, C.R. Foster, G. Guiochon, J. Chromatogr. A 761 (1997) 41.
[16] G. Guiochon, T. Farkas, H. Guan-Sajonz, J.-H. Koh, M. Sarker, B.J. Stanley, T. Yong, J. Chromatogr. A 762 (1997) 83.
[17] J.-H. Koh, G. Guiochon, J. Chromatogr. A 796 (1998) 41.
[18] J.H. Koh, B.S. Broyles, H. Guan-Sajonz, M.Z.C. Hu, G. Guiochon, J. Chromatogr. A 813 (1998) 223.
[19] G. Guiochon, E. Drumm, D. Cherrak, J. Chromatogr. A 835 (1999) 41.
[20] M. Sarker, G. Guiochon, J. Chromatogr. A 683 (1994) 293.
[21] G. Carta, W.B. Stringfield, J. Chromatogr. A 658 (1994) 407.
[22] D.P. Gervais, W.S. Laughinghouse, G. Carta, J. Chromatogr. A 708 (1995) 41.
[23] J.H. Knox, G.R. Laird, P.A. Raven, J. Chromatogr. 122 (1976) 129.
[24] J.E. Baur, E.W. Kristensen, R.M. Wightman, Anal. Chem. 60 (1988) 2334.
[25] T. Farkas, M.J. Sepaniak, G. Guiochon, AIChE J. 43 (1997) 1964.
[26] T. Farkas, G. Guiochon, Anal. Chem. 69 (1997) 4592.
[27] R.P. Zou, A.B. Yu, Chem. Eng. Sci. 50 (1995) 1504.
[28] R.P. Zou, A.B. Yu, Chem. Eng. Sci. 51 (1996) 1177.
[29] R. Di Felice, E. Parodi, AIChE J. 42 (1996) 927.
[30] K.C.E. Ostergen, A.C. Tragardh, G.G. Enstad, J. Mosby, AIChE J. 44 (1998) 1.
[31] C.R. Wilke, P. Chang, AIChE J. 1 (1955) 264.
[32] J.J. Van Deemter, F.J. Zuiderweg, A. Klinkenberg, Chem. Eng. Sci. 5 (1956) 271.
[33] D.W. Taylor, Fundamentals of Soil Mechanics, Wiley, New York, 1948.
[34] T.W. Lambe, R.V. Whitman, Soil Mechanics. SI Version, Wiley, New York, 1979.
[35] B.G. Yew, E.C. Drum, G. Guiochon, Simulation of Wall Friction Effects in High Performance Liquid Chromatography (HPLC) Columns. Proceedings of the Fourth International Conference on Constitutive Laws for Engineering Materials: Experiment, Theory, Computation and Applications, Troy, NY, 1999, pp. 513–516.
[36] D. Train, J. Pharm. Pharmacol. 8 (1956) 745.
[37] R.B. Bird, W.E. Stewart, E.N. Lightfoot, Transport Phenomena, Wiley, New York, 1960.
[38] H. Guan, G. Guiochon, J. Chromatogr. A 731 (1996) 27.
[39] B.G. Yew, E. Drumm, G. Guiochon, manuscript in preparation.
[40] K. Mihlbachler, T. Kollmann, A. Seidel-Morgenstern, J. Tomas, G. Guiochon, J. Chromatogr. A 818 (1998) 155.
[41] J. Krim, Sci. Am. 275 (No. 4) (1996) 74.
[42] J. Krim, Surface Sci. 500 (2001) in press.
[43] P. Weiss, Sci. News 158 (2000) 56.
[44] Y. Braiman, F. Family, H.G.E. Hentschel, C. Mak, J. Krim, Phys. Rev. E 59 (1999) R4737.